Attosecond electro-optic effect in zinc sulfide induced by a laser field

T. Otobe

Kansai Photon Science Institute, National Institutes for Quantum and Radiological Science and Technology, 8-1-7, Umemidai, Kizugawa City, Kyoto 619-0215, Japan

(Received 24 February 2019; published 3 September 2019)

An ultrafast electro-optic effect of the zinc sulfide crystal is predicted employing a numerical pump-probe simulation. The numerical results indicate that the time dependence of the off-diagonal part of the dielectric function of ZnS exhibits a phase shift with respect to the pump laser field. The phase shift coincides with the time-resolved dynamical Franz-Keldysh effect, which is the modulation of the isotropic part of the dielectric function. While the probe frequency dependence around the band gap is not intense, it becomes intense at higher photon energies of approximately 42 eV.

DOI: 10.1103/PhysRevA.100.033401

I. INTRODUCTION

In the past two decades, advances in laser sciences and technologies have led to the availability of intense coherent light sources with different characteristics. Ultrashort laser pulses can be as short as a few tens of attoseconds, leading to the development of the field of attosecond science [1]. Intense laser pulses of midinfrared (MIR) or terahertz (THz) frequencies have also recently become available [2,3]. By employing these extreme sources of coherent light, investigating the optical response of materials in real-time with suboptical cycle resolution is possible [1,4–8].

The dielectric function $\varepsilon_{\alpha\beta}(\omega)$ is the most fundamental quantity characterizing the optical properties of matter. The dielectric function observed in an ultrafast pump-probe experiment can be further considered as a probe time (T_p)-dependent function, $\varepsilon_{\alpha\beta}(T_p, \omega)$. We determined the subcycle change in the optical properties, i.e., the time-resolved dynamical Franz-Keldysh effect (Tr-DFKE), which corresponds to the response of the dressed states and quantum path interference of different dressed states [9–13]. In particular, this ultrafast change exhibits an interesting phase shift that depends on the field amplitude and probe frequency. By utilizing this phenomenon, we can develop an ultrafast optical modulator or an ultrafast optical switch.

Recently, the Tr-DFKE was experimentally observed by a near-infrared (NIR) -pump extreme-ultraviolet (EUV) -probe with attosecond time resolution for polycrystalline diamond [14,15]. A similar effect was also observed in an excitonic state in a GaAs quantum well by THz-pump NIR-probe spectroscopy [16]. However, because the signal by the Tr-DFKE is small, a high-precision measurement or an intense pump field is required.

The diagonal parts $\varepsilon_{\alpha\alpha}$ represent the ordinary optical response, whereas the off-diagonal parts $\varepsilon_{\alpha\beta}$ ($\alpha \neq \beta$) represent the rotation of the light polarization. Because the off-diagonal parts can be detected as the polarization direction, it is sensitive to the change of signal. The magnetic field and electric field can induce off-diagonal parts. An ultrafast optical Faraday effect induced by the circular laser field has been proposed theoretically [17]. Under the electric field, some material shows an intense electro-optic effect, e.g., the Pockels effect and the Kerr effect. The electro-optic effect is utilized to probe the waveform of the THz field and ultrafast phenomena such as laser-accelerated electron bunch [18].

The Pockels effect induced by the modulation of the crystal structure on the picosecond timescale is strong and is thus frequently employed. In contrast, the electro-optic effect on the atto- or femtosecond timescale is attributed to electron dynamics. The electro-optic effect of materials under an intense laser field on the attosecond timescale may differ from the electro-optic effect at longer timescales because the diagonal part of dielectric function $\varepsilon_{\alpha\alpha}$ is modulated nonadiabatically. In this study, we want to demonstrate the ultrafast electro-optic effect in the attosecond time domain by employing time-dependent density functional theory (TDDFT). We assume ZnS as the target material, which is a typical electro-optic material.

II. COMPUTATIONAL METHOD

To derive time-dependent conductivity, we will revisit a simple model that we reported in our previous work [11]. The probe's electric field is assumed to be weak enough that it can be represented by linear-response theory. We denote the electric current caused by the probe field as $J_p(t)$, which is assumed to be parallel to the direction of the probe's electric field. Its relationship to the time-domain conductivity $\sigma(t, t')$ is given as

$$J^p_\alpha(t) = \int_{-\infty}^{t} dt' \sigma_{\alpha\beta}(t, t') E^p_\beta(t'), \tag{1}$$

where $E_p(t')$ is the electric field of the probe pulse. We note that the conductivity $\sigma(t, t')$ depends on both times t and t' rather than just the time difference $t - t'$ due to the presence of the pump pulse.

The ultrashort probe pulse field can be assumed as

$$E^p(t) = E^p_0 \sin[\omega_p(t - T_p)] \exp[-(t - T_p)^2/2\eta^2], \tag{2}$$

 ©2019 American Physical Society

where ω_p is the frequency, E_0^p is the peak field intensity, η is the pulse duration, and T_p is the probe time. If the probe laser duration is much shorter than the optical cycle of the pump laser, we can define the time-dependent conductivity, $\tilde{\sigma}_{\alpha\beta}(T_p, \omega)$, as

$$\tilde{\sigma}_{\alpha,\beta}(T_p, \omega) = \frac{\int dt\, e^{i\omega t} J_\alpha^p(t)}{\int dt\, e^{i\omega t} E_\beta^p(t)}. \tag{3}$$

We use the real-time TDDFT program package SALMON [19]. The details of the computational methods have been reported elsewhere [11,20,21]. We describe the electron dynamics in a unit cell of a crystalline solid under a spatially uniform time-varying electric field $E(t)$. Treating the field as a vector potential $\vec{A}(t) = -c\int^t dt'\vec{E}(t')$, the electron dynamics are described by the time-dependent Kohn-Sham (TDKS) equation [22]. We use a norm-conserving pseudopotential for the electron-ion potential [23,24]. For the exchange-correlation potential, we employ an adiabatic local density approximation (LDA) [25]. The cubic unit cell containing four zinc atoms and four sulfur atoms was discretized into Cartesian grids of 24^3. The k space also discretized into 16^3 grid points.

In practice, we use the following electric fields. The pump field is of the form

$$E_P(t) = -E_{0,P} f_P(t) \cos \Omega t \tag{4}$$

whose direction is along the [001] axis. The envelope is $f_P(t) = \cos^2(\frac{\pi}{2\zeta_P} t)$ for $-\zeta_P < t < \zeta_P$ and $f_P(t) = 0$ for $|t| \geqslant \zeta_P$.

The probe field is oriented in the [100] direction. The field strength of the probe pulse is set to $E_0^p = 2.7 \times 10^{-3}$ MV/cm, which is small enough to probe the linear response of the medium.

It should be noted that the TDDFT does not include the dephasing and the relaxation, which comes from the scattering and/or photoemission. Therefore, the induced current lasts permanently after the excitation takes place. To calculate the conductivity at T_p, we change Eq. (3) to

$$\tilde{\sigma}_{\alpha,\beta}(T_p, \omega) = \frac{\int dt\, e^{i\omega t} G(t) J_\alpha^p(t)}{\int dt\, e^{i\omega t} E_\beta^p(t)}. \tag{5}$$

Here, $G(t)$ is the window function,

$$G(t) = e^{-(t-T_p)^2/\tau^2}, \tag{6}$$

to reduce the unphysical Fourier component, which comes from the finite current at the end of the time evolution.

III. NUMERICAL RESULTS

A. Around the band gap

Typical calculation results are shown in Fig. 1. This calculation takes 14 h with 256 Xeon E5-2680 v3 processors. Figure 1(a) shows the electric field in the [001] (pump) and [100] (probe) directions. The frequency of the pump field, Ω, is 0.775 eV, and the pulse duration is 21.3 fs. The probe pulse duration (η) is set to 0.707 fs, and the center frequency is $\omega_p = 2$ eV. Although the probe pulse duration looks too short to realize in experiment, the pulse duration should be much shorter than the optical cycle of the pump laser to see the subcycle response around the band gap. Figure 1(b) shows the induced current. The dashed red line and solid blue line represent the diagonal and off-diagonal current, respectively. Figure 2 shows the real and imaginary parts of ε_{xx} with (dashed lines) and without (solid lines) the pump field calculated from the results shown in Fig. 1. In this calculation, we use a sufficiently long gate time, $\tau = 3$ fs, for the gate function [Eq. (6)] to avoid the artificial modulation.

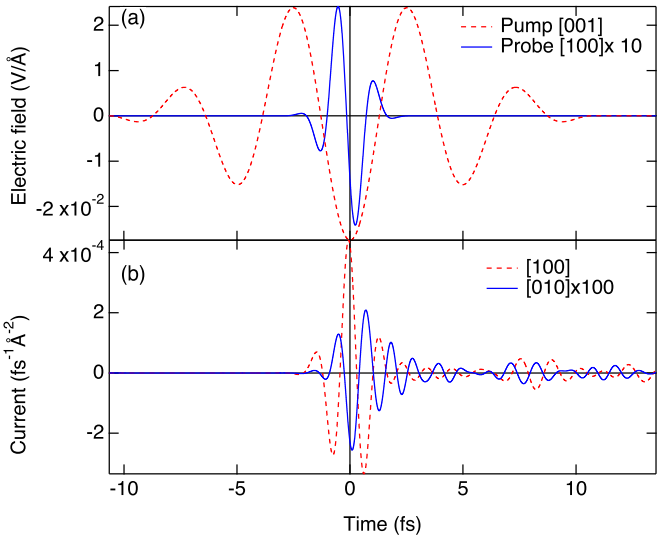

FIG. 1. (a) Pump (red dashed line) and probe field (blue line) as a function of time. The polarization of the pump pulse is parallel to the [001] (z) direction and that of the probe pulse is parallel to the [100] (x) direction. (b) Electronic current induced parallel (red dashed line) and orthogonal (blue solid line) to the probe pulse polarization.

Figure 3 shows the difference between ε with and without the pump fields. The red lines present the diagonal part, $\Delta\varepsilon_{xx}(T_p, \omega)$, and the blue lines present the off-diagonal part, $\varepsilon_{yx}(T_p, \omega)$, which are induced by the pump laser field. $\Delta\varepsilon_{xx}(T_p, \omega)$ is large around 4 eV, which corresponds to the intense absorption above the band gap (red lines in Fig. 2). This result indicates that the Tr-DFKE and off-diagonal modulation in ε are intense at 4 eV, whereas diamond shows intense modulation around the optical band gap [11].

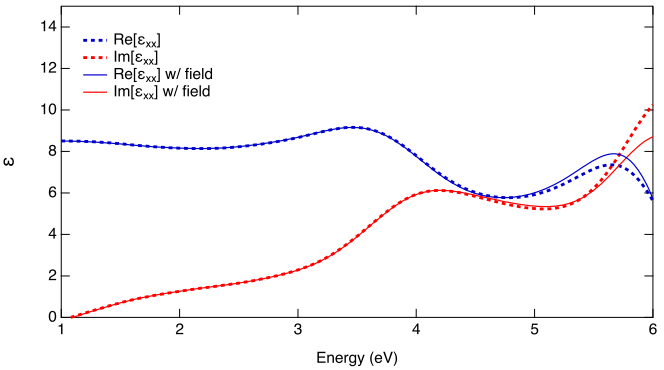

FIG. 2. Dielectric function of ZnS with and without the pump field. The probe time (T_p) is 0 fs.

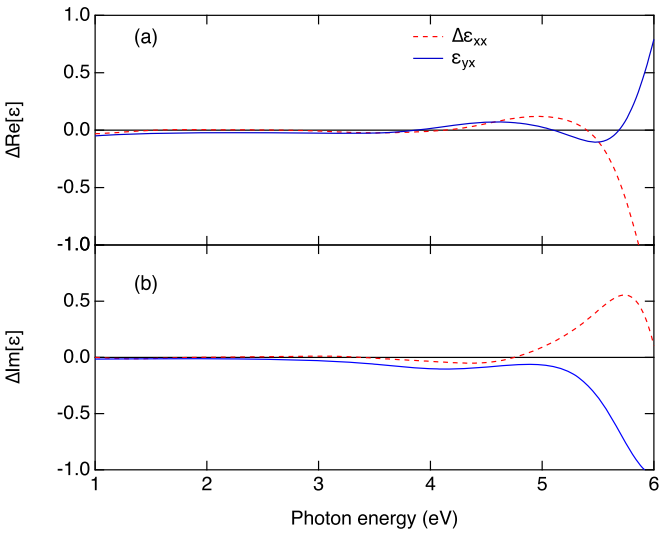

FIG. 3. Modulation of the diagonal (red dashed line) and off-diagonal part (blue solid line) of the dielectric function.

The time dependence of $\Delta\varepsilon(T_p, \omega)$ is shown in Fig. 4. The color scale in the energy above 5 eV is 20 times wider than below it, because the signal becomes so intense that the modulation around the gap cannot be distinguished. ZnS shows intense modulation above 4 eV where intense photoabsorption occurs. The off-diagonal part ε_{yx} shows odd-order response with respect to the pump electric field at each energy, whereas the $\Delta\varepsilon_{xx}$ has even order due to the Tr-DFKE [11]. This result indicates that the direction of the pump field switches the sign of ε_{yx}, which is qualitatively the same as odd-order nonlinear

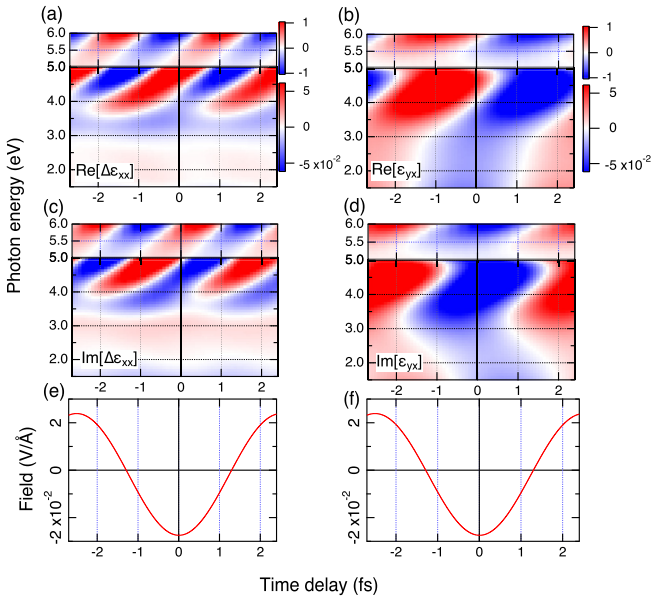

FIG. 4. Time-resolved modulation of the dielectric function, $\varepsilon_{\alpha\beta}(T_p, \omega)$. The peak intensity of the pump laser is 1×10^{10} W/cm^2 with a frequency of $\Omega = 0.775$ eV. (a),(b) The real parts of $\Delta\varepsilon_{xx}(T_p, \omega)$ and $\varepsilon_{yx}(T_p, \omega)$. (c),(d) The imaginary parts of $\Delta\varepsilon_{xx}(T_p, \omega)$ and $\varepsilon_{yx}(T_p, \omega)$. (e),(f) Pump field at the probe time delay.

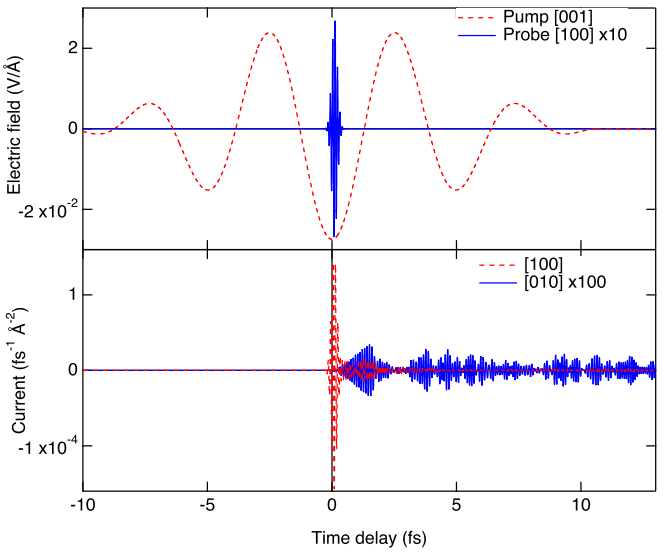

FIG. 5. Upper: Pump (red dashed line) and probe (blue line) fields as a function of time. The polarization of the pump pulse is parallel to the [001] (z) direction and the probe pulse is parallel to the [100] (x) direction. Lower: Electronic current induced parallel (red line) and orthogonal (blue dotted line) to the probe pulse polarization.

effects whose lowest order is the Pockels effect. There is a kink in ε_{yx} around 5.5 eV, which cannot be seen in $\Delta\varepsilon_{xx}$.

From the familiar formula for the Pockels effect for the cubic system, in the adiabatic limit, the off-diagonal refractive index coincides with the pump laser field. From previous works on the Tr-DFKE, $\Delta\varepsilon_{xx}(T_p)$ oscillates in even harmonic orders of Ω, i.e., $e^{i2m\Omega T_p}$. Then, ε_{yx} shows the modulation with odd harmonics, $e^{i(2m\pm1)\Omega T_p}$.

Although the Pockels-like effect below 3 eV coincides with the phase of the pump laser field, the photon energy dependence in Figs. 4(b) and 4(d) indicates a nonadiabatic response above 3.5 eV. The phase shift of $\varepsilon_{yx}(T_p, \omega)$ with respect to ω is similar to that of $\Delta\varepsilon_{xx}(T_p, \omega)$. The ω-dependent phase shift in $\Delta\varepsilon_{xx}(T_p, \omega)$ corresponds to the relative phase of two Floquet states at T_p [11–13,16]. Therefore, the ω-dependent phase indicates that the Pockels-like effect in the nonadiabatic regime is also the result of the relative phase between the Floquet states.

B. High photon energy region

In the previous calculations, we showed the nonadiabatic subcycle response in the off-diagonal dielectric function in the vicinity of the band gap. However, sub-fs pulses in the VUV region have not been utilized. As the next step, we would like to show the subcycle response of $\varepsilon_{yx}(T_p, \omega)$ around the photon energy of 42 eV [14]. In the case of the lower-energy probe, interaction between a few bands may be dominant. In particular, around the band gap, $\mathrm{Re}[\varepsilon_{yx}(T_p, \omega)]$ shows the usual Pockels-like-effect adiabatic response. On the other hand, in the higher photon energy region, a response complicated by the contribution of many bands is expected.

Figure 5 shows (a) the pump and probe fields and (b) the induced current in the [100] and [010] directions. The pulse duration η is set to $\eta = 0.11$ fs. The current by the

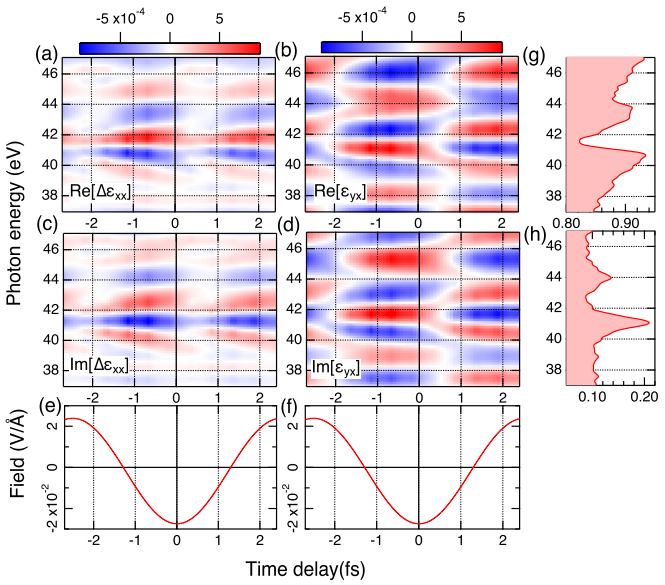

FIG. 6. Time-resolved modulation of the dielectric function, $\varepsilon_{\alpha\beta}(T_p, \omega)$. The center frequency of probe light (ω_p) is 42 eV. (a),(b) The real part of the $\Delta\varepsilon_{xx}(T_p, \omega)$ and $\varepsilon_{yx}(T_p, \omega)$. (c),(d) The imaginary part of $\Delta\varepsilon_{xx}(T_p, \omega)$ and $\varepsilon_{yx}(T_p, \omega)$. (e),(f) Pump field at the probe time delay. (g),(h) The real and imaginary part of ε_{xx} without pump field. The real and imaginary parts of ε_{xx} without pump field are shown in (g) and (h).

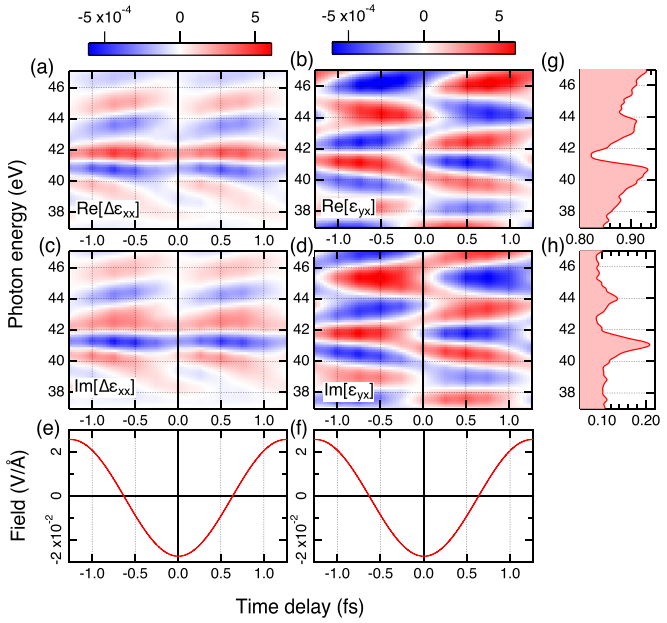

FIG. 7. Time-resolved $\Delta\varepsilon_{\alpha\beta}(T_p, \omega)$. The peak intensity of the pump laser is 1×10^{10} W/cm^2 with a frequency of $\Omega = 1.6$ eV.

off-diagonal part (the current in the [010] direction) shows a slow increase compared to the case of low frequency [Fig. 1(b)]. We set $\tau = 2$ fs to include the peak of the current around 2 fs in Fig. 5(b).

The $\varepsilon(T_p, \omega)$ is shown in Fig. 6. The diagonal part, $\Delta\varepsilon_{xx}(T_p, \omega)$, indicates that Tr-DFKE occurs around 41 eV, which corresponds to the peak of the absorption without the pump field [Figs. 6(g) and 6(h)]. Although the off-diagonal part, $\varepsilon_{yx}(T_p, \omega)$ [Figs. 6(b) and 6(d)], indicates odd-harmonic oscillation with respect to the pump laser field, as we expected, the direction of the light rotation is strongly dependent on the photon energy. The $\varepsilon_{yx}(T_p, \omega)$ also indicates an intense phase shift with respect to the pump field, which coincides with the phase of the Tr-DFKE [$\Delta\varepsilon_{xx}(T_p, \omega)$]. These photon energy and time-delay dependencies do not appear in the low-frequency probe.

The Pockels-like response is expected to be sensitive to the pump laser frequency (Ω), because the photon energy and delay-time dependence of $\varepsilon_{yx}(T_p, \omega)$ appear to be affected by that of $\varepsilon_{xx}(T_p, \omega)$. Figure 7 shows the case of $\Omega = 1.6$ eV. Since the frequency is increased, the dynamical effect in $\varepsilon(T_p, \omega)$ should be enhanced compare to that of Fig. 6.

The $\varepsilon_{yx}(T_p, \omega)$ and $\Delta\varepsilon_{xx}(T_p, \omega)$ show the maximum when $E_P = 0$ V/Å. This behavior is similar to the Tr-DFKE with a weak pump laser field in diamond [11]. With respect to the photon energy dependence, $\Delta\varepsilon_{xx}(T_p, \omega)$ in Fig. 7 shows a different dependence from Fig. 6, because the energies of the Floquet states are different. On the contrary, the $\varepsilon_{yx}(T_p, \omega)$ shows almost the same photon energy dependence as that of Fig. 6.

These results for the high-frequency probe case indicate that the anisotropic response including many electronic bands shows more complicated behavior than the Tr-DFKE and the low-frequency case.

IV. SUMMARY

In this study, we demonstrated the ultrafast Pockels-like response in ZnS on the attosecond timescale using time-dependent density functional theory. Our results demonstrate the usual adiabatic response around the band gap. Conversely, for the higher probe frequency, ε_{yx} shows a significant dependence on the probe frequency and time. In particular, the time dependence coincides with the phase of the Tr-DFKE. Because detecting the anisotropic response is sensitive to the modulation, it may be a good candidate for the ultrafast optical switching device.

ACKNOWLEDGMENTS

This work was supported by JST-CREST under Grant No. JP-MJCR16N5, and by JSPS KAKENHI, Japan Grants No. 15H03674 and No. JP17H03525. Numerical calculations were performed on the supercomputer SGI ICE X at the Japan Atomic Energy Agency.

[1] M. Hentschel, R. Kienberger, C. Spielmann, G. A. Reider, N. Milosevic, T. Brabec, P. Corkum, U. Heinzmann, M. Drescher, and F. Krausz, Nature (London) **414**, 509 (2001).

[2] H. Hirori, A. Doi, F. Blanchard, and K. Tanaka, Appl. Phys. Lett. **98**, 091106 (2011).

[3] A. H. Chin, O. G. Calderón, and J. Kono, Phys. Rev. Lett. **86**, 3292 (2001).

[4] H. Hirori, K. Shinokita, M. Shirai, S. Tani, Y. Kadoya, and K. Tanaka, Nat. Commun. **2**, 594 (2011).
[5] A. Schiffrin, T. Paasch-Colberg, N. Karpowicz, V. Apalkov, D. Gerster, S. Mühlbrandt, M. Korbman, J. Reichert, M. Schultze, S. Holzner, J. V. Barth, R. Kienberger, R. Ernstorfer, V. S. Yakovlev, M. I. Stockman, and F. Krausz, Nature (London) **493**, 70 (2012).
[6] M. Schultze, E. M. Bothschafter, A. Sommer, S. Holzner, W. Schweinberger, M. Fiess, M. Hofstetter, R. Kienberger, V. Apalkov, V. S. Yakovlev, M. I. Stockman, and F. Krausz, Nature (London) **493**, 75 (2012).
[7] M. Schultze, K. Ramasesha, C. Pemmaraju, S. Sato, D. Whitmore, A. Gandman, J. S. Prell, L. J. Borja, D. Prendergast, K. Yabana, D. M. Neumark, and S. R. Leone, Science **346**, 1348 (2014).
[8] F. Novelli, D. Fausti, F. Giusti, F. Parmigiani, and M. Hoffmann, Sci. Rep. **3**, 1227 (2013).
[9] A. P. Jauho and K. Johnsen, Phys. Rev. Lett. **76**, 4576 (1996).
[10] K. B. Nordstrom, K. Johnsen, S. J. Allen, A.-P. Jauho, B. Birnir, J. Kono, T. Noda, H. Akiyama, and H. Sakaki, Phys. Rev. Lett. **81**, 457 (1998).
[11] T. Otobe, Y. Shinohara, S. A. Sato, and K. Yabana, Phys. Rev. B **93**, 045124 (2016).
[12] T. Otobe, Phys. Rev. B **94**, 165152 (2016).
[13] T. Otobe, Phys. Rev. B **96**, 235115 (2017).
[14] M. Lucchini, S. A. Sato, A. Ludwig, J. Herrmann, M. Volkov, L. Kasmi, Y. Shinohara, K. Yabana, L. Gallmann, and U. Keller, Science **353**, 916 (2016).
[15] F. Schlaepfer, M. Lucchini, S. A. Sato, M. Volkov, L. Kasmi, N. Hartmann, A. Rubio, L. Gallmann, and U. Keller, Nat. Phys. **14**, 560 (2018).
[16] K. Uchida, T. Otobe, T. Mochizuki, C. Kim, M. Yoshita, H. Akiyama, L. N. Pfeiffer, K. W. West, K. Tanaka, and H. Hirori, Phys. Rev. Lett. **117**, 277402 (2016).
[17] M. S. Wismer, M. I. Stockman, and V. S. Yakovlev, Phys. Rev. B **96**, 224301 (2017).
[18] M. Nishiura, Z. Yoshida, T. Mushiake, Y. Kawazura, R. Osawa, K. Fujinami, Y. Yano, H. Saitoh, M. Yamasaki, A. Kashyap, N. Takahashi, M. Nakatsuka, and A. Fukuyama, Rev. Sci. Instrum. **88**, 023501 (2017).
[19] M. Noda, S. A. Sato, Y. Hirokawa, M. Uemoto, T. Takeuchi, S. Yamada, A. Yamada, Y. Shinohara, M. Yamaguchi, K. Iida, I. Floss, T. Otobe, K.-M. Lee, K. Ishimura, T. Boku, G. F. Bertsch, K. Nobusada, and K. Yabana, Comput. Phys. Commun. **235**, 356 (2019).
[20] G. F. Bertsch, J.-I. Iwata, A. Rubio, and K. Yabana, Phys. Rev. B **62**, 7998 (2000).
[21] T. Otobe, M. Yamagiwa, J.-I. Iwata, K. Yabana, T. Nakatsukasa, and G. F. Bertsch, Phys. Rev. B **77**, 165104 (2008).
[22] E. Runge and E. K. U. Gross, Phys. Rev. Lett. **52**, 997 (1984).
[23] N. Troullier and J. L. Martins, Phys. Rev. B **43**, 1993 (1991).
[24] L. Kleinman and D. M. Bylander, Phys. Rev. Lett. **48**, 1425 (1982).
[25] J. P. Perdew and A. Zunger, Phys. Rev. B **23**, 5048 (1981).